ERJ Express. Published on July 22, 2010 as doi: 10.1183/09031936.00086410

Lymphatic and blood microvasculature organization in pulmonary sarcoid granulomas

Running head: Microvascularization in sarcoid granulomas

Marianne Kambouchner,[1] Daniel Pirici,[2] Jean-François Uhl,[3] Laurentiu Mogoanta,[2] Dominique Valeyre,[4] Jean-François Bernaudin[5]

[1]Department of Pathology, Hôpital Avicenne, AP–HP, Université Paris 13, 93009 Bobigny Cedex, France;

[2]Department of Histology, University of Medicine and Pharmacy, Craiova, Romania;

[3]URDIA, Service d'Anatomie Biomédicale des Saints Pères, Université Paris 5, 75006 Paris, France;

[4]Department of Pulmonary Medicine, Hôpital Avicenne, AP–HP, Université Paris 13, 93009 Bobigny Cedex, France;

[5]Laboratory of Histology and Tumor Biology, Hôpital Tenon, AP–HP and ER2 Université Paris 6, 75020 Paris, France.

Correspondence to:

Dr M Kambouchner at the address given above; e-mail: marianne.kambouchner@avc.aphp.fr; fax number: +33(0)148955602; phone number: +33(0)148955604

Keywords: lymphatics, microvessels, fibrosis, sarcoid granulomas

ABSTRACT

Question of the study: Pulmonary sarcoid granulomas are characterized by their elective distribution along collecting lymphatics. However, relationships between granulomas and intralobular lymphatics or blood microvascularization have not been investigated. Therefore, we undertook a specific analysis of blood capillaries and lymphatics supplying sarcoid granulomas to identify additional clues to understanding the pathophysiogenesis of these lesions.

Materials and Methods: Six pulmonary samples were immunolabeled with D2-40, anti-CD34 and anti-CD31 antibodies, paying particular attention to the relationships between lymphatics and granulomas, and the pattern of blood microvessels supplying sarcoid lesions. A morphometric study of granulomas included their distance to lymphatics, and a 3D-reconstruction of a granuloma in its lymphatic context.

Results: Intralobular granulomas were closely associated with lymphatics; apart from a few granulomas, blood capillaries stopped at the outer border of the fibrous ring surrounding granulomas, and perigranuloma capillaries were particularly scarce.

Answer to the question: Our observations of the lymphatic and blood microvascular environment of intralobular pulmonary sarcoid granulomas provide evidence for the critical role of lymphatics in the emergence of these lesions. Moreover, pulmonary sarcoid lesions could be considered avascular structures, thereby providing new insights into the understanding of the granuloma physiology and the distribution of blood-borne therapeutic agents.

INTRODUCTION

Sarcoidosis is a multisystem disorder of unknown cause with thoracic involvement in up to 90% of patients.[1] Sarcoid granulomas are comprised of clusters of epithelioid and giant cells surrounded by a rim of lymphocytes and fibroblasts. A peripheral fibrous ring of varied thickness later surrounds the lesions that have a tendency to coalesce, resulting in typical fibrotic nodules. The characteristic distribution of granulomas along the pulmonary collecting lymphatics, ie, peribronchovascular spaces, interlobular septa and subpleural connective tissue, is a major diagnostic criterion.[2] Moreover, their tropism for the outer wall of pulmonary arteries or veins is well known.[3]

In addition to these features, the relationships between pulmonary sarcoid granulomas and, respectively, the intralobular lymphatic network or the pulmonary blood capillaries have not yet been adequately examined. Investigating these close relationships might help improve our understanding the biology of granulomas and also orient therapeutic drug research to achieve better targeted distribution. To address this issue, we systematically analyzed the interface between granulomas and the lymphatic network by means of D2-40 immunohistochemical labeling or their blood microvessels with CD34 and CD31 immunolabeling.[4,5] To better discriminate their blood and lymphatic vascular supplies, we specifically focused our study on selected isolated granulomas, whose location is predominantly intralobular.

MATERIALS AND METHODS

Surgical lung biopsies

Surgical lung biopsies from 6 patients (1 woman and 5 men; age range: 29–53 years) with pulmonary sarcoidosis referred to our Pulmonary Department were retrieved from the files of the Department of Pathology. These tissue specimens were selected because of the presence

of multiple, well-defined, sarcoid granulomas scattered throughout the pulmonary parenchyma.

This retrospective study was conducted in accordance with French legislation concerning medical research.

Tissue-section processing

Five μm-thick tissue sections were stained with hematoxylin–eosin and Masson's trichrome stains. For immunohistochemistry studies, sections were incubated with mouse monoclonal IgG antibodies to D2-40, which recognizes podoplanin expressed by lymphatic vascular endothelium, anti-CD31, which recognizes platelet endothelial cell adhesion molecule-1, and anti-CD34, which recognizes a 115-kDa transmembrane glycoprotein.[4,5] The latter two are expressed on blood vascular endothelial cells.[5] Forty serial sections from one specimen were incubated only with D2-40 for the 3D-study.

Immunolabeling was processed as previously described using an automated procedure (Ventana Medical Systems, Tucson, AZ). Antigen retrieval was achieved by boiling at 95–100°C. Anti-D2-40 (Dako, Trappes, France; clone 07 3611; 1/100 dilution; concentration 0.25 $mg.l^{-1}$) was incubated for 32 min at 37°C. Anti-CD34 (Dako; clone 96 3820 B; 1/100 dilution; concentration 0.5 $mg.l^{-1}$) was incubated for 60 min at 42°C, and anti-CD31 (Dako; clone JC70A; 1/20 dilution; concentration 515 $mg.l^{-1}$) was incubated for 20 min at 37°C. Sections were then incubated with the biotinylated universal anti-mouse immunoglobulin secondary antibody (Ventana SA, Illkirch, France) for 16 min at 37°C, followed by incubation with the avidin–biotin–horseradish peroxidase complex using the Ventana Medical Systems Basic DAB detection kit for 8 min at 37°C. The final revelation system (Dako DMKiVIEW DAB) used horseradish peroxidase–diaminobenzidine as the final chromogen.

As negative controls, sections from each specimen were incubated with a normal mouse IgG1 (Dako; X0931 culture supernatant) instead of the primary antibody. Slides were counterstained with hematoxylin.

Microscopy analysis

We focused our observations on sarcoid granulomas located within the intralobular parenchyma, as non-aggregated, isolated granulomas are mostly found in this area. Microscopy analysis comprised two steps. First, the D2-40–labeled sections were screened and digitalized, and labeled lymphatic vessels in the vicinity of each granuloma were counted. D2-40–labeled lymphatics were identified as structures with an open or collapsed lumen, but with a clearly visible endothelial layer. A total of 311 sarcoid granulomas (mean of 54 granulomas per lung section) was studied, 249 of which were located within the pulmonary lobules and 62 along interlobular septa. The morphometric analysis was pursued on a set of 38 digitized images from the microscopy analysis.

Second, the distribution of blood microvessels associated with granulomas was analyzed using CD34- and CD31-immunolabeled sections. We recorded the presence or absence of associated CD31-labeled blood vessels in each section and counted the number of present on a set of 85 strictly intralobular granulomas, which were selected from among those described above precisely because they were isolated, ie, non-aggregated early lesions that are easier to examine thoroughly.

Morphometric analysis

Morphometric analyses were conducted on a set of 38 digitized images of non-coalesced, isolated granulomas adjacent to D2-40–positive vessels. All images were processed using Nikon NIS-Elements software (Nikon, Apidrag, Bucharest, Romania). The respective areas

(A), perimeters (P), and minimum and maximum diameters were then calculated. A script was recorded and automatically run for each image to generate each granuloma's center of gravity, referred to as the "centroid". The sphericity index (SI) was calculated as the d_1/d_2 ratio ($d_1 = 2\sqrt{A/\pi}$; $d_2 = P/\pi$), equal to 1 when the structure is a perfect circle, ie, the cross-section of a sphere. The respective shortest distances from adjacent lymphatics to the proximal border and the "centroid" of the granulomas were then calculated manually.

All data were exported and analyzed in Excel (Microsoft Corporation, Redmond, WA, USA).

3D-reconstruction of lymphatic–granuloma relationships

A granuloma – located within the lobular parenchyma with a diameter not exceeding 1 mm so as to be completely visible on all serial sections and easy to follow – was selected for 3D-reconstruction. Twelve consecutive D2-40–immunolabeled sections were selected and digitized using Aperio's ScanScope system (Aperio; Vista, CA, USA). Segmentation was obtained by manually drawing the boundaries of the four main components: ie, clusters of epithelioid cells, the surrounding connective tissue, D2-40–labeled lymphatics and a small satellite artery. The consecutive images were then loaded into WinSurf (SURF driver 4.0; http://www.surfdriver.com), producing a vectorial 3D model featuring the coalescent granulomas and their adjacent lymphatics.

RESULTS

Morphology of sarcoid granulomas

Typical histopathological features of pulmonary florid sarcoidosis were observed in all six lung biopsies: ie, compact, non-caseating epithelioid and giant-cell granulomas predominantly located near peribronchovascular bundles, interlobular septa, and along the subpleural

connective tissue, but also within the lobular parenchyma, which was examined in particular detail. Few intralobular granulomas close to or within the alveolar spaces were devoid of a fibrotic ring, while most were surrounded by connective tissue stained blue by Masson's trichrome, suggesting a high type I collagen content (fig 1).

The distributions of the respective minimum and maximum diameters for a set of 38 intralobular granulomas (fig 2) demonstrated a minimum diameter exceeding 200 μm in up to 37% of them. Analysis respectively the area and perimeter of granulomas evaluated by the mean ± standard deviation SI (0.86 ± 0.07) confirmed the constant spheroid-like "rugby ball" or ellipsoid form of the lesions.

Lymphatic network–granuloma relationship

Analysis of the D2-40–immunolabeled sections (table 1) showed that most granulomas (59% and 74% of intralobular and perilobular granulomas, respectively) were adjacent to at least one small lymphatic. The presence of labeled lymphatics in the vicinity of intralobular granulomas is illustrated in fig 3. Two or more lymphatics were associated with up to 27% of intralobular granulomas, suggesting their woven basket-like arrangement around granulomas.

The distance between the closest lymphatic wall and the granuloma border was less than 20 μm for up to 65% of intralobular sarcoid granulomas (mean: 33 ± 51 μm; range: 0–256 μm). The distance between the "granuloma centroid" and the next lymphatic wall exceeded 150 μm for 63% of the lesions (mean: 182 ± 97 μm; range: 23–431 μm). No lymphatic vessel was seen within granulomas.

3D-reconstruction of a sarcoid granuloma and its surrounding lymphatic network

The 3D-reconstruction model (fig 4) clearly illustrates the internal structure of a sarcoid granuloma which consists of small clusters of closely packed epithelioid and giant cells

surrounded by a connective tissue sheath traversed by the lymphatic network. No lymphatic was observed within the cellular part of the granuloma.

Blood microvascular network–granuloma relationship

Other than a few juxta-alveolar granulomas, blood capillaries were rarely seen in the vicinity of granulomas (fig 3). The CD34- or CD31-labeled blood-microvessel network of the interalveolar walls was stopped in contact with the outer fibrous ring of sarcoid granulomas. Because CD31 labeling of juxta-granuloma blood vessels was more intense than CD34 labeling, quantitative analysis was performed on CD31-immunolabeled sections, analyzing 85 granulomas and their environment. CD31-labeled blood microvessels were observed only in 15% of the granulomas, at the periphery of the perigranuloma fibrous ring. A larger CD31-positive blood vessel, identified as an intralobular vein or artery, weakly immunolabeled for CD34, was seen close to the perigranuloma fibrous ring of 25% of intralobular granulomas; therefore, at least 75% of granulomas were devoid of blood vessels in their immediate vicinity.

No blood capillary or larger vessel was seen in either the central part of granulomas or their outer fibrous ring.

DISCUSSION

The lymphatic distribution of pulmonary sarcoid granulomas is a well-known and constant histopathological feature of sarcoidosis and thus serves as a valuable diagnostic criterion for it.[2,6] However, until now, the intimate morphological relationships between pulmonary sarcoid granulomas and the lymphatic network had never been analyzed in detail. On another hand, although the tropism of pulmonary sarcoid granulomas for the blood vessel walls has been widely described, little is known about the pattern of the blood microvessel supply in the

immediate vicinity of sarcoid granulomas.[3] We thought that better comprehension of the relationships between individual sarcoid lesions and their lymphatic or blood microvascular networks might provide insights into the pathophysiology of the disease and help design future therapeutics.

Using samples of pulmonary surgical biopsies, we first demonstrated that most of the intra- and perilobular sarcoid granulomas were associated with at least one lymphatic. Notably, the scattered intralobular granulomas were connected to the lymphatic network, supporting the hypothesis of the critical role of lymphatics in the pathophysiology of the disease. Second, CD31 and CD34 immunolabeling of the same samples showed that the granulomas were very poorly supplied by blood capillaries at the outer edge of the peripheral fibrous ring, far from the cellular compartment.

In most open lung biopsies taken in the setting of pulmonary sarcoidosis, granulomas surrounded by fibrotic rings coalesced to form a nodule, thereby perturbing the topographic lobular distribution of lesions. Therefore, to obtain a meticulous evaluation of the topographic markings of each granuloma, we intentionally focused our study on solitary lesions usually observed within the intralobular parenchyma, away from the sarcoid nodules. It is important to keep in mind that the technological advances of immunohistochemistry only recently enabled the thin lymphatic network supplying the collecting lymphatics to be described in detail.[4]

Pulmonary lymphatics play a pivotal role in regulating the drainage of alveolar fluids throughout the interstitial framework under physiological conditions and following lung injury.[7–9] Importantly, a wide range of small particles including organic and inorganic dusts, and infectious microorganisms, are processed and drained by the lymphatics reaching the collecting channels located within perivenular and peribroncho-arterial sheaths.[7–9] Indeed, some studies particularly emphasized the major role of the lymphatics in granuloma

formation after alveolar processing of airborne pathogens. In guinea pigs experimentally infected by aerosols containing *Mycobacterium tuberculosis*, it was demonstrated that the thin connective tissue space between the alveolar membrane and the lymphatic was the selective area for inflammatory cell clustering, giving rise to epithelioid and giant-cell granulomas.[10] The role of airborne environmental factors in the pathogenesis of pulmonary sarcoidosis is strongly suspected.[11–15] A prospective study conducted on patients diagnosed with pulmonary sarcoidosis revealed a link with beryllium exposure in a significant percentage of them.[16] Moreover, a relationship between sarcoidosis and exposure to the crystalline silica cristobalite was demonstrated in the population of an Icelandic district.[11] Similarly, sarcoid-like pulmonary granulomatosis has been reported in New York firefighters, following the World Trade Center Disaster.[12] More recently, specific attention was paid to the role of pulmonary lymphatics in the clearance of inhaled ultrafine and nanosized particles <100 nm.[22] In contrast with larger particles, once deposited, these nanoparticles readily translocate to extrapulmonary sites.[17] Indeed, it could be tempting to suggest the role of such particles as a triggering factor in the granulomatous process of sarcoidosis, a systemic disease with major pulmonary and node involvement.

We did not observe any lymphatics within granulomas. Although the walls of lymphatics constantly adhered to the thin fibrotic ring enveloping granulomas, lymphatic lumens seem to have merely been displaced from their native course by sarcoid lesions. Morphometric data on SI and the distances from the granuloma "centroid" to the closest lymphatic vessels support this type of granulomatous concentric growth in contact with, but not integrating lymphatics. Similarly, a previous ultrastructural study performed on serial ultra-thin sections containing a pulmonary sarcoid granuloma, identified a lymphatic within the peripheral connective tissue, but none within the granulomatous cell component.[18] Those authors described the presence of lymphocytes and mononuclear cells within this

lymphatic running along the outside of the perigranuloma fibrous ring, but the direction of its flow could not be determined.[18] Granulomas are composed of central clusters of epithelioid cells and giant cells primarily associated with peripheral T lymphocytes.[19] All those observations strongly support a major role of juxta-granuloma lymphatics in lymphocyte-trafficking towards mediastinal lymph nodes. The mobilization of $CD4^+$ T lymphocytes, known to play a pivotal role in the granulomatous process of sarcoidosis via the lymphatics might explain the onset of granulomas along the lymphatic collectors flowing towards the mediastinal lymph nodes.[19]

Except for a very few small-diameter granulomas localized in the interalveolar walls, capillary CD31 and CD34 immunolabeling showed blood microvascularization confined at the outer border of the connective tissue ring, far from the cellular compartment in up to 85% of sarcoid granulomas. This finding suggests that a large majority of pulmonary sarcoid granulomas can be considered “avascular”. Those observations, along with previous findings, give rise to three hypotheses. First, we did not observe any angiogenesis in pulmonary sarcoidosis, in contrast with other pulmonary inflammatory fibrotic processes.[20] This absence of angiogenesis is at variance with the expected findings, in light of the high levels of vascular endothelial growth factor in bronchoalveolar lavage fluids reported in sarcoidosis, and in epithelioid cells detected by immunohistochemistry and *in-situ* hybridization.[21,22] Conversely, macrophages are also known to secrete antiangiogenic factors, such as endostatin/collagen XVIII.[23] However, the secretion of such factors by epithelioid or giant cells has not been reported.

Second, more than half of the granulomas we examined exceeded 200 μm in diameter, leading us to think that the distance separating them from the blood capillaries could be responsible for intragranuloma hypoxia. Indeed, it was shown that the pO_2 gradient in tissues dropped exponentially as a function of the distance from the blood vessels.[24] In the present

context, such a hypothetical relationship between the granuloma pO_2 gradient and the distance from blood vessels and/or alveolar spaces could be advanced. The evidence suggests that the center of aggregated granulomas, impacted in a thick fibrous sheath is much further from the blood vessels, and therefore even more hypoxic. The concept of "hypoxic granuloma" in sarcoidosis is supported by previously described hypoxemic granulomas in the setting of experimental tuberculosis in guinea pigs.[25] Such a hypothesis could also explain, at least in part, perigranuloma fibrosis, the hallmark of sarcoid granuloma progression.[2,6,26–29] In this hypoxic context, transforming growth factor-β, one of the cytokines secreted by sarcoid granulomas, has been shown to exert a synergistic action on collagen production by fibroblasts.[28,29] Moreover, it is striking that a minority of small diameter interalveolar granulomas close to blood capillaries or alveolar spaces were not associated with a fibrous ring.

Third, the distance between capillaries and the cellular component of granulomas might hamper the distribution of systematically administered drugs used to treat sarcoidosis. Indeed, a collagen-rich area including a well-defined collagen network organized like a "capsule" was demonstrated to facilitate the interstitial transport of fluid and molecules.[30]

In conclusion, this focused examination of the morphological features of the local lymphatic environment of intralobular pulmonary sarcoid granulomas provided new evidence for the critical role of lymphatics in the emergence of these lesions, and reinforced the putative role of airborne particles in their pathogenesis. Furthermore, the consequences of the scarce blood microvessels on the role of hypoxia in granulomas or impairment of therapeutic drug distribution can be envisaged.

Acknowledgments

We are grateful to Lydie Germain and Brigitte Lejeune for their technical help and to Prof. Antoine Martin, Prof. Patrice Callard and “Amis du Centre des Tumeurs de Tenon” (ACTT) for their constant support. The authors thank Janet Jacobson for editorial assistance.

REFERENCES

1. Iannuzzi MC, Rybicki BA, Teirstein AS. Sarcoidosis. *N Engl J Med* 2007; 357: 2153-2156

2. Travis MD, Colby TV, Koss MN, Rosado-de-Christenson ML, Müller NL, King TE. Atlas of non tumor pathology 2. Non neoplastic disorders of the lower respiratory tract. 1st Edn. Washington, DC: Armed Forces Institute of Pathology. 2002: pp123-136.

3. Takemura T, Matsui Y, Saiki S, Mikami R. Pulmonary vascular involvement in sarcoidosis. *Hum Pathol* 1992; 23:1216-1223.

4. Kambouchner M, Bernaudin JF. Intralobular pulmonary lymphatic distribution in normal human lung using D2-40 antipodoplanin immunostaining. *J Histochem Cytochem* 2009; 57: 643-648.

5. Pusztaszeri MP, Seelentag W, Bosman FT. Immunohistochemical expression of endothelial markers CD31, CD34, von Willebrand factor, and Fli-1 in normal human tissues. *J Histochem Cytochem* 2006; 54: 385-395.

6. Ma YL, Gal A, Koss MN. The pathology of pulmonary sarcoidosis: update. *Semin Diagn Pathol* 2007; 24: 150-161.

7. Leak LV. Lymphatic removal of fluids and particles in the mammalian lung. *Environ Health Perspect* 1980; 35: 55-75.

8. Lauweryns JM, Baert JH. Alveolar clearance and the role of the pulmonary lymphatics. *Am Rev Respir Dis* 1977; 115: 625-683.

9. Macklin C. Lung fluid, alveolar dust drift and initial lesions of disease in the lung. *CMAJ* 1955; 72: 664-665.

10. Basaraba RJ, Smith EE, Shanley CA, Orme IM. Pulmonary lymphatics are primary sites of *Mycobacterium tuberculosis* infection in guinea pigs infected by aerosol. *Infect Immun* 2006; 74: 5397-5401.

11. Rafnsson V, Ingmarsson O, Hjalmarsson I, Gunnarsdottir H. Association between exposure to crystalline silica and risk of sarcoidosis. *Occup Environ Med* 1998; 55: 657-660.

12. Izbicki G, Chavko R, Banauch GI, Weiden MD, Berger KI, Aldrich TK, Hall C, Kelly KJ, Prezant DJ. World Trade Center "sarcoid-like" granulomatous pulmonary disease in New York City Fire Department rescue workers. *Chest* 2007; 131:1414-1423.

13. American Thoracic Society, European Respiratory Society, World Association of Sarcoidosis and Other Granulomatous Disorders. Statement on sarcoidosis. *Am J Respir Crit Care Med* 1999; 160: 736-755.

14. Martin WJ, Iannuzzi MC, Gail DB, Peavy HH. Future directions in sarcoidosis research. Summary of an NHLBI working group. *Am J Respir Crit Care Med* 2004; 170: 567-571.

15. Jajosky P. Sarcoidosis diagnoses among US military personnel: trends and ship assignment associations *Am J Prev Med* 1998; 14: 176-183.

16. Müller-Quernheim J, Gaede KI, Fireman E, Zissel G. Diagnosis of chronic beryllium disease within cohorts of sarcoidosis patients. *Eur Respir J* 2006; 27: 1190-1195.

17. Oberdörster G, Oberdörster E, Oberdörster J. Nanotoxicology: an emerging discipline evolving from studies of ultrafine particles. *Environ Health Perspect* 2005; 113: 823-839.

18. Soler P, Basset F, Bernaudin JF, Chrétien J. Morphology and distribution of the cells of a sarcoid granuloma: ultrastructural study of serial sections. *Ann N Y Acad Sci* 1976; 278: 147-

160.

19. Grunewald J, Eklund A Role of $CD4^+$ T cells in sarcoidosis. State of the art *Proc Am Thorac Soc* 2007; 4: 461-464.

20. Tzouvelekis A, Anevlavis S, Bouros D. Angiogenesis in interstitial lung diseases: a pathogenetic hallmark or a bystander? *Respir Res* 2006; 7: 82.

21. Vasakova M, Sterclova M, Kolesar L, Slavcev A, Pohunek P, Sulc J, Skibova J, Striz I. Bronchoalveolar lavage fluid: cellular characteristics, functional parameters and cytokine and chemokine levels in interstitial lung diseases. *Scand J Immunol* 2009; 69: 268-274.

22. Tolnay E, Kuhnen C, Voss B, Wiethege T, Müller KM. Expression and localization of vascular endothelial growth factor and its receptor *FLT* in pulmonary sarcoidosis. *Virchows Arch* 1998; 432: 61-65.

23. Paddenberg R, Faulhammer P, Goldenberg A, Kummer W. Hypoxia-induced increase of endostatin in murine aorta and lung. *Histochem Cell Biol* 2006; 251: 497-508.

24. Torres Filho IV, Leuning M, Yuan F, Intaglietta M, Jain RK.Non invasive measurement of microvascular and interstitial oxygen profiles in a human tumor in SCID mice. *Proc Natl Acad Sci U S A* 1994; 91: 2081-2085.

25. Via LE, Lin PL, Ray SM, Carrillo J, Allen SS, Eum SY, Taylor K, Klein E, Manjunatha U, Gonzales J, Lee EG, Park SK, Raleigh JA, Cho SN, McMurray DN, Flynn JL, Barry CE. Tuberculous granulomas are hypoxic in guinea pigs, rabbits and non-human primates. *Infect Immun* 2008; 76: 2333-2340.

26. Higgins DF, Kimura K, Iwano M, Haase V. Hypoxia-inducible factor signalling in the

development of tissue fibrosis. *Cell Cycle* 2008; 7: 1128-1132.

27. Tzouvelekis A, Harokopos V, Paparountas T, Oikonomou N, Chatziioannou A, Vilaras G, Tsiambas E, Karameris A, Bouros D, Aidinis V. Comparative expression profiling in pulmonary fibrosis suggests a role of hypoxia-inducible factor-1alpha in disease pathogenesis. *Am J Respir Crit Care Med* 2007; 176: 1108-1119.

28. Falanga V, Zhou L, Yufit T. Low oxygen tension stimulates collagen synthesis and COL1A1 transcription through the action of TGF-beta1. *J Cell Physiol* 2002; 191: 42-50.

29. Salez F, Gosset P, Copin MC, Lamblin Degros C, Tonnel AB, Wallaert B. Transforming growth factor-beta1 in sarcoidosis. *Eur Respir J* 1998; 12: 913-919.

30. Netti PA, Berk DA, Swartz MA, Grodzinsky AJ, Jain RK. Role of extracellular matrix assembly in interstitial transport in solid tumors. *Cancer Res* 2000; 60: 2497-2503.

Table 1: Relationship between D2-40–labeled lymphatics and intralobular or perilobular sarcoid granulomas. Results are expressed as n (%) of granulomas associated with at least one lymphatic (total), according to the number of lymphatics observed.

	Granulomas	
No. of associated D2-40 lymphatics	**Intralobular (n = 249)**	**Perilobular (n = 62)**
1	80 (32%)	26 (42%)
2	37 (15%)	11 (18%)
3	17 (7%)	8 (13%)
≥4	12 (5%)	1 (1%)
total	147 (59%)	46 (74%)

Figure legends

Figure 1 Examples of hematoxylin–eosin (A, B) or Masson's trichrome (C, D) staining of intralobular pulmonary sarcoid granulomas. Note the dense blue-stained surrounding two granulomas in Figure 1D (magnifications: A ×350; B ×250; C ×400; D ×250).

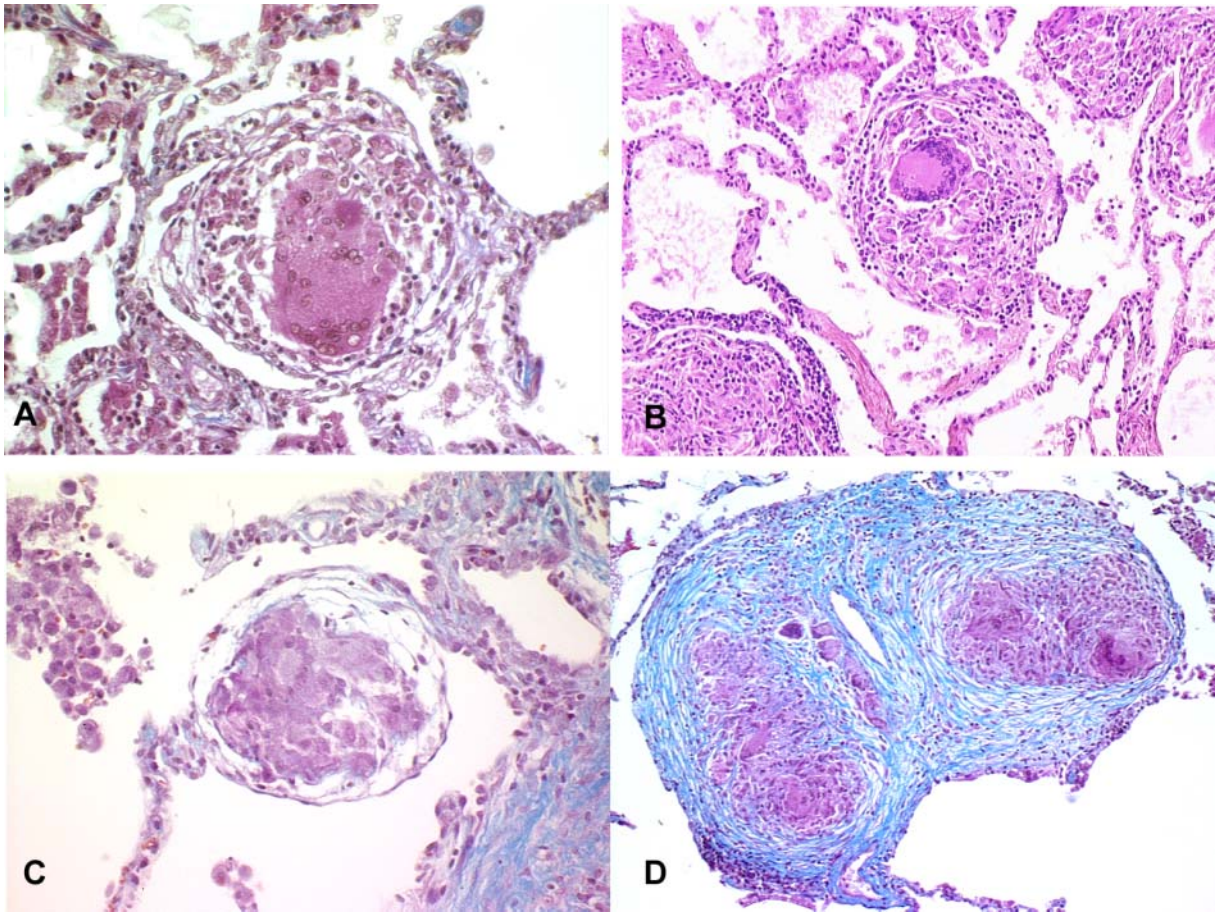

Figure 2 Morphometric analysis of the respective minimal (minimal D) and maximal (maximal D) diameters expressed in µm (y axis) of 38 intralobular pulmonary sarcoid granulomas (x axis).

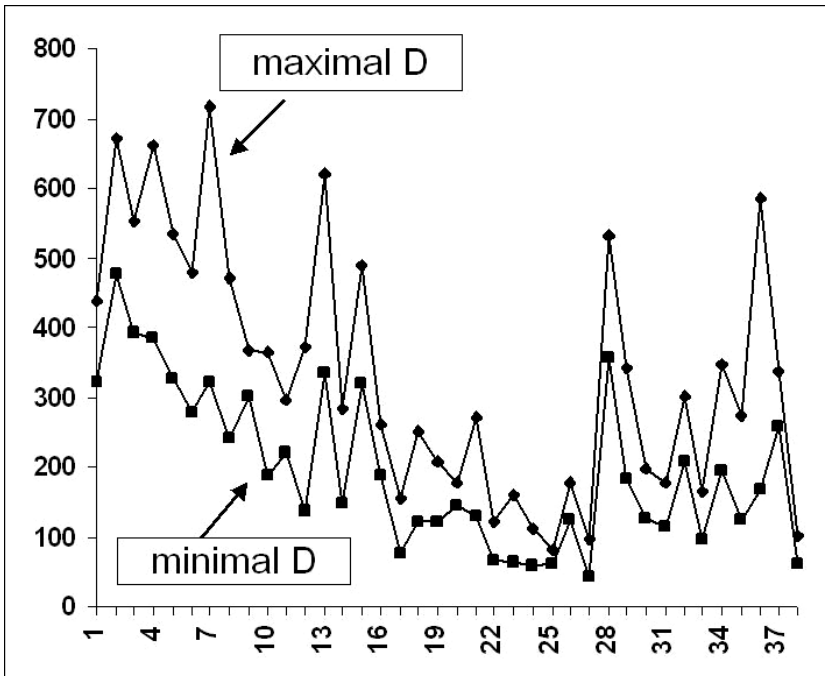

Figure 2

Figure 3 Lymphatic (L: A, B, C) and blood microvessels (*: D, E, F) associated with intralobular sarcoid granulomas. A and B (magnification ×350) and (C) (magnification ×500) show D2-40–labeled lymphatics near granulomas. (D) (magnification ×300) and (E) (magnification ×400) show CD34 immunolabeling of blood capillaries. Note the intense CD34 labeling of alveolar capillaries. (F) (magnification ×350) shows CD31 immunolabeling of a larger blood vessel. Note the absence of small blood capillaries close to the granulomas.

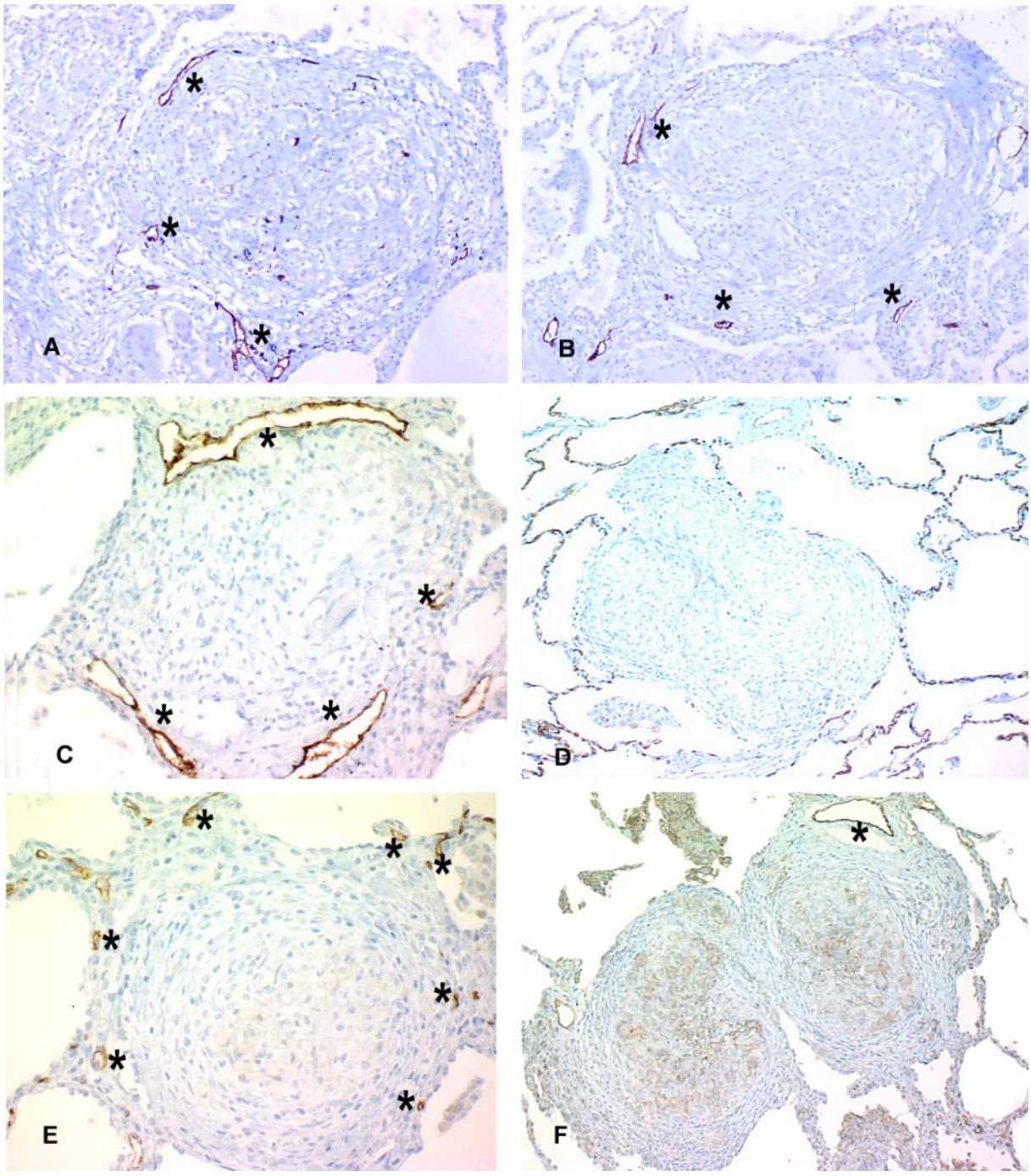

Figure 4 3D-reconstruction of granulomas located within a pulmonary lobule. Twelve D2-40–immunolabeled serial sections were used for 3D modeling of the lesion. The clusters of the cellular components of granulomas (G) are pink, whereas the surrounding connective tissue sheath (F) is purple. D2-40–labeled lymphatic channels (L) and lymphatic collectors (C) are yellow and the satellite intralobular artery (A) is blue.

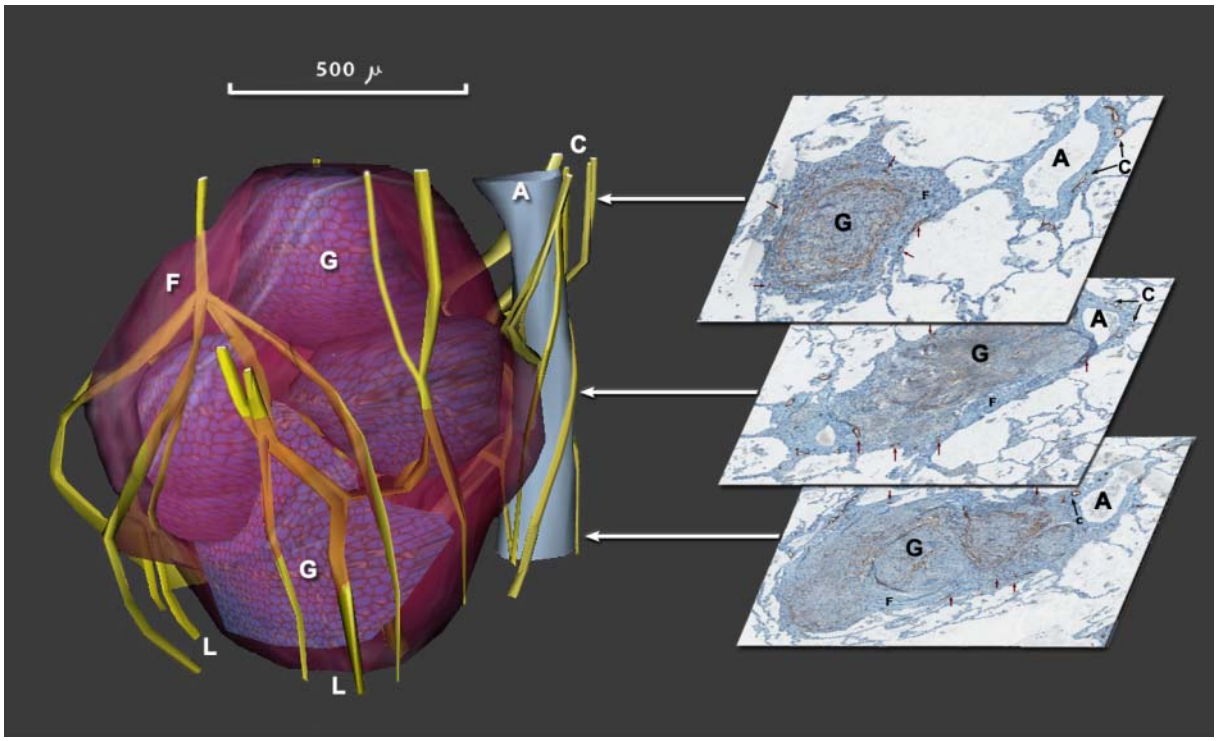
500 µ
C
A
F
G
G
L
L
A
C
G
F
A
C
G
F
A
C
G
F